Proc. Natl. Acad. Sci. USA
Vol. 93, pp. 8671–8676, August 1996
Neurobiology

Norepinephrine transporters have channel modes of conduction

AURELIO GALLI, RANDY D. BLAKELY, AND LOUIS J. DEFELICE*

Department of Pharmacology, Vanderbilt University School of Medicine, Nashville TN 37232-6600

Communicated by Ronald H. Kaback, University of California, Los Angeles, CA, April 25, 1996 (received for review October 17, 1995)

ABSTRACT **Neurotransmitter transporters couple to existing ion gradients to achieve reuptake of transmitter into presynaptic terminals. For coupled cotransport, substrates and ions cross the membrane in fixed stoichiometry. This is in contrast to ion channels, which carry an arbitrary number of ions depending on the channel open time. Members of the γ-aminobutyric acid transporter gene family presumably function with fixed stoichiometry in which a set number of ions cotransport with one transmitter molecule. Here we report channel-like events from a presumably fixed stoichiometry [norepinephrine (NE)$^+$, Na^+, and Cl^-], human NE (hNET) in the γ-aminobutyric acid transporter gene family. These events are stimulated by NE and by guanethidine, an hNET substrate, and they are blocked by cocaine and the antidepressant desipramine. Voltage-clamp data combined with NE uptake data from these same cells indicate that hNETs have two functional modes of conduction: a classical transporter mode (T-mode) and a novel channel mode (C-mode). Both T-mode and C-mode are gated by the same substrates and antagonized by the same blockers. T-mode is putatively electrogenic because the transmitter and cotransported ions sum to one net charge. However, C-mode carries virtually all of the transmitter-induced current, even though it occurs with low probability. This is because each C-mode opening transports hundreds of charges per event. The existence of a channel mode of conduction in a previously established fixed-stoichiometry transporter suggests the appearance of an aqueous pore through the transporter protein during the transport cycle and may have significance for transporter regulation.**

Monoamine transporters make up an important subclass of the γ-aminobutyric acid transporter gene family (1, 2). They regulate the action of catecholamines and serotonin by maintaining appropriate concentrations of the transmitter for receptors in the central and peripheral nervous systems. Monoamine transporters are the targets for cocaine, antidepressants, and amphetamines that profoundly affect chemical signaling in central and peripheral nervous synapses. These transporters presumably reside in presynaptic terminal membranes, where they recycle transmitters for subsequent release (3). Noradrenergic transporters, such as norepinephrine transporters (NETs), terminate noradrenergic transmission at postganglionic sympathetic synapses and may contribute to ischemic efflux of norepinephrine (NE), leading to cardiac arrhythmias (4). Monoamine transporters also exist in the placenta, where they assist in transplacental transfer of amines, and in blood platelets, where they regulate blood levels of serotonin. Thus, understanding the mechanism of monoamine transport (5–7) may shed light on both regulatory and pathological mechanisms related to amine clearance. Since catecholamine transporters were first discovered over three decades ago (8–12), the study of their mechanism has relied almost exclusively on the uptake of radioactive ligands (13–19). From these studies it is well known that NETs saturate at submicromolar NE concentrations and that they require millimolar concentrations of Na and Cl to function. Furthermore, NETs have a specific requirement for Na such that even similar ions, like Li, cannot substitute for Na. Nevertheless, NETs recognize and transport structurally similar substrates including epinephrine, dopamine, amphetamines, and guanethidine (GU). Radioligand uptake studies on resealed membrane vesicles from NET-containing cells indicate that NETs function through the stoichiometric transport of NE, Na, and Cl, whereby Na and Cl move down their electrochemical gradients to concentrate NE. The predicted stoichiometry of one NE^+, one Na^+, and one Cl^- indicates the net transfer of one positive charge per transport cycle. At the measured uptake velocity of approximately one NE per second, these studies would, by a naive calculation, lead to an elementary current far below the resolution of available biophysical techniques. Indeed, 10^6 transporters working in unison would yield a current of less than 0.2 pA. Although other transporters have higher turnover rates that may yield larger currents, members of the γ-aminobutyric acid transporter gene family have low stoichiometric flux rates similar to NETs (5). Thus previous studies of electrogenic transport in the γ-aminobutyric acid transporter family predict extremely small transporter currents, even under saturating conditions of the transmitter and the cotransported ions. With the availability of cDNA clones for specific amine transporters, it is now possible to record currents from populations of NE transporters. We have expressed human NETs (hNETs) at a high density in HEK-293 (human embryonic kidney) cells and have recorded the electrical response to transmitters using the patch-clamp technique. Transfected cells generate currents the order of −100 pA at −100 mV (20), well above the predicted amount. This inward current saturates with NE concentration (30 μM) but not with membrane voltage. Similar data have been obtained for the structurally homologous transporters for γ-aminobutyric acid, serotonin, and glutamate (21–28). None of these previous experiments, however, have explained the transmitter-induced currents and fluctuations in terms of elementary events. The present study is an attempt to demonstrate and quantify the underlying events responsible for NE-induced currents in cells transfected with human NE transporters.

METHODS

Stable Cell Lines. An *XhoI*/*XbaI* fragment containing the complete hNET cDNA (29) was released from pBluescript SKII− (Stratagene) and subcloned into *XhoI*/*XbaI*-digested pcDNA3 (Invitrogen), placing hNET expression under control of the cytomegalovirus promoter and the T7 RNA polymerase promoter. To generate stably-transfected cells, hNET/pcDNA3 was transfected by Lipofectin (Life Technologies, Grand Island, NY) into HEK-293 cells at 50–60% confluency in Dulbecco's Modified Eagle Medium with 10% heat-inactivated fetal bovine serum, 100 μg of penicillin per ml, and 100 units of streptomycin per ml. After 3 days, parental and transfected cells were switched to a medium containing 250 μg

The publication costs of this article were defrayed in part by page charge payment. This article must therefore be hereby marked "*advertisement*" in accordance with 18 U.S.C. §1734 solely to indicate this fact.

Abbreviations: NE, norepinephrine; NET, NE transporter; GU, guanethidine; DS, desipramine; C-mode, channel mode.

*To whom reprint requests should be addressed.

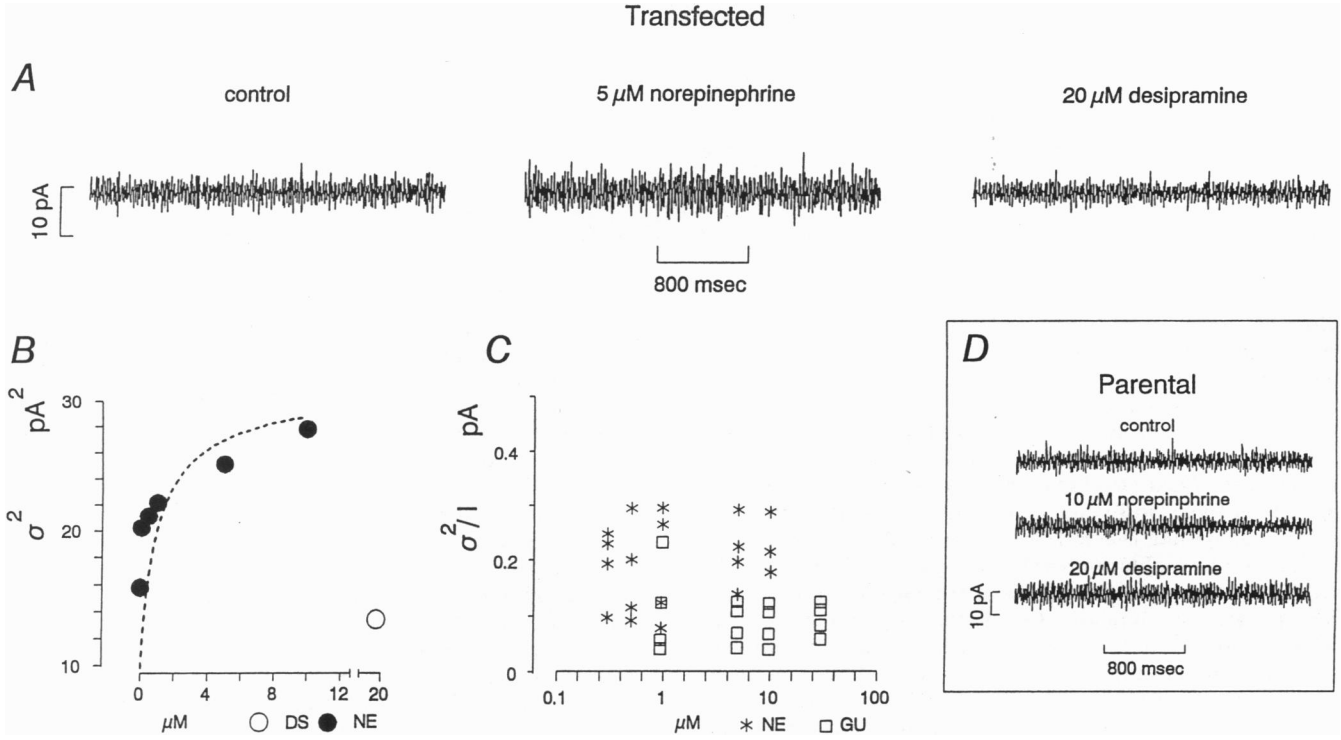

FIG. 1. Whole-cell current fluctuations. NE induces current fluctuations in hNET-transfected HEK-293 cells. (*A*) Three current traces (steady-state current subtracted) at −120 mV (2000 Hz bandwidth). The traces show current fluctuations before adding NE (*Left*), after adding 5 μM NE (*Center*), and after adding 20 μM DS (*Right*). (The IC_{50} of DS for the NE-induced current is 68 nM; Galli *et al.*, ref. 20). (*B*) Plots of the difference variance of the current fluctuations for a typical experiment. $\sigma^2 = \sigma^2_{NE} - \sigma^2_{DS}$ plotted as a function of the concentration of NE used to induce the current. The variance of the induced, DS-sensitive fluctuations obeys the empirical relationship $\sigma^2 = \sigma^2_{max}[NE]^n/(K_M{}^n + [NE]^n)$. The dashed line in *B* is this expression for σ^2, with $\sigma^2_{max} = 29.5$ pA², $K_M = 0.61$ μM, and $n = 0.9$. The average for four cells gave $\sigma^2_{max} = 31 \pm 3$ pA², $K_M = 0.60 \pm 0.13$ μM, and $n = 0.80 \pm 0.15$. GU-induced fluctuations follow a similar pattern with $\sigma^2_{max} = 25.0 \pm 2.5$ pA², $K_M = 0.61 \pm 0.40$ μM, and $n = 1.40 \pm 0.15$ (4 cells). (*C*) Ratio of difference variance ($\sigma^2 = \sigma^2_{NE} - \sigma^2_{DS}$) to the mean difference current ($I = I_{NE} - I_{DS}$) for NE (stars; four cells) and for GU (squares; 4 cells). A regression analysis of σ^2/I against the substrate concentration gives a mean ratio of 0.18 ± 0.04 pA for NE and 0.11 ± 0.02 pA for GU. The value of the variance-to-mean ratio for the combined NE and GU data is 0.145 ± 0.045 pA. *C* indicates no correlation between the variance-to-mean ratio and the concentration on the transmitter. (*D*) Parental cells are unaffected by NE or DS. Concentrations of up to 30 μM of NE, GU, or DS have no effect on parental cells (20).

of geneticin (G418) per ml; resistant colonies were isolated from transfected plates 1 week later. Single cells were used to generate clonal lines. Multiple lines tested positive for desipramine (DS)-sensitive [³H]NE uptake. Clonal line 293-hNET-#3 (termed 293-hNET cells) was used in all experiments reported here. 293-hNET cells (20) express an 80-kDa protein detected by the affinity-purified antipeptide NET antibody from N430 cells (30). The binding of a high-affinity cocaine analogue [^{125}I]3β-[4-iodophenyl]tropan-2β-carboxylic acid methyl ester to total cell membrane preparations gave a value of $K_D = 14.2 \pm 1.6$ nM, Hill coefficient $n = 0.96 \pm 0.10$, and $B_{max} = 13.1 \pm 0.6$ pmol/mg of protein. (Throughout the paper, ± refers to the standard deviation associated with a fit to the data.) These binding experiments indicate a single population of noninteracting transporter sites with an average of 9×10^5 binding sites per cell (20). Although we do not know exact number of NETs in any particular cell, in the present paper, we approximate this as 10^6 NETs per cell. Finally, the uptake of [³H]NE follows Michaelis–Menten kinetics with $K_M = 420 \pm 38$ nM, Hill coefficient $n = 1.3 \pm 0.1$, and $V_{max} = 5.2 \pm 0.1 \times 10^{-17}$ mol/cell per min at 37°C.

Electrophysiology. Before recording from parental or stably transfected cells, cells were plated at 10^5 per 35-mm culture dish. Attached cells were washed three times with bath solution at 37°C. The bath contained the following: 130 mM NaCl, 1.3 mM KCl, 1.3 mM KH_2PO_4, 0.5 mM $MgSO_2$, 1.5 mM $CaCl_2$, 10 mM Hepes, and 34 mM dextrose. Pipette solutions for the whole-cell recording contained the following: 130 mM KCl, 0.1 mM $CaCl_2$, 2 mM $MgCl_2$, 1.1 mM EGTA, 10 mM Hepes, and 30 mM dextrose adjusted to pH 7.35 and 270 mosmol; free Ca was 0.1 μM. To prevent NE oxidation, solutions contained 100 μM pargyline and 100 μM ascorbic acid. Patch electrodes (5 MΩ) were pulled from borosilicate glass (Corning 7052). An Axopatch 200A amplifier (Axon Instruments, Foster City, CA) band-limited with a four-pole Butterworth filter (Ithaca, Ithaca, NY) at 2000 Hz was used to measure current. Series conductance was 0.1 uS or greater, and cell capacitance was 25–80 pF, implying 2500–8000 μm² surface area. Voltage steps (500 msec) ranging from −140 to 0 mV, were separated by −40 mV holding potentials (1 sec). Data were stored digitally on VCR and analyzed on a Nicolet 4094 oscilloscope and an IBM-AT computer.

RESULTS AND DISCUSSION

Here we present evidence that the relatively large transmitter-induced current present in transfected cells can be ascribed to a channel-like behavior associated with hNETs. As already noted, either NE or the false transmitter GU can induce currents in hNET-transfected HEK-293 cells (20). The NE-induced currents, which are blocked by DS and cocaine, obey the equation

$$I = I_{max}[NE]^n/(K_M{}^n + [NE]^n)$$

for fixed negative voltage. At −120 mV and 130 mM Na, $I_{max(NE)} = 49 \pm 19$ pA, $K_{M(NE)} = 0.60 \pm 0.04$ μM, and Hill coefficient $n = 1.02 \pm 0.06$. At −120 mV and in 30 μM NE, $K_{M(Na)} = 15.0 \pm 3.0$ mM and $n_{Na} = 1.1 \pm 0.2$. $I_{max(GU)}$ varies linearly in the range −20 through −40 mV, and the whole-cell

resistance defined by DS subtraction was 1.11 ± 0.12 GΩ. GU-induced currents follow a similar pattern, although on average, the GU-induced currents are larger than the NE-induced currents. At −120 mV and 130 mM Na, $I_{max(GU)}$ = 117 ± 36 pA, $K_{M(GU)}$ = 2.4 ± 0.3 μM, and n_{GU} = 1.10 ± 0.14. The Hill coefficients for NE, GU, and Na evaluated from the induced currents are approximately equal to one, which is close to the value obtained from uptake assays. We have also measured the binding of a cocaine analogue to assess the number of transporters, yielding an average of ≈10^6 hNETs per transfected cell (see *Methods*). With these data, and considering NE as a monovalent cation and GU as a trivalent cation, $I_{max(NE)}/B_{max}$ gives a cycle rate of 340 cycles/sec and $I_{max(GU)}/B_{max}$ gives 270 cycles/sec at −120 mV. These values are considerably higher than the rates measured from our uptake studies on these same cells (20), for which V_{max}/B_{max} gives less than 1 NE/sec per hNET, in agreement with the literature value. Thus, whereas transmitter-induced currents from hNETs appear to have a stoichiometry similar to uptake, the NE-induced currents at −120 mV (48 pA) are ≈300 times too large compared with current that is expected from transport, assuming the formula $I = Nqr$, where N is the number of transporters per cell (10^6), q is the net transfer of charge per turnover (1 e), and r is the turnover rate (one per second). One possible explanation for the discrepancy between the rates determined from uptake studies and the rates determined from induced currents may be inherent differences in the two techniques. In single-cell voltage clamp experiments, we intentionally select cells with large currents, whereas uptake experiments average over thousands of cells, some of which may have low expression or be nonfunctional. Thus uptake studies may underestimate the rates. Alternatively, the rate of transfer determined by the two methods may result from different transport mechanism within the transporter, one for NE and the other for ions that may permeate hNET through a transporter-associated pore. The charge transported through such a pore might be expected to be much larger than charge-transported by hNET via the fixed stoichiometry $NE^+:Na^+:Cl^-$.

To examine this latter possibility, we first investigated the elementary events that underlie the transmitter-induced current using fluctuation analysis. If the unitary charge transfer is 200–300 times larger than predicted by fixed stoichiometry, this could explain the discrepancy in rates measured by NE uptake and rates measured by NE-induced current. Fig. 1*A* illustrates the current fluctuations in hNET-transfected HEK-293 cells voltage clamped to −120 mV. In this figure, the steady current was suppressed and the fluctuations were limited to 2000 Hz bandwidth. To quantify the evident increase in the DS-sensitive, NE-induced fluctuations (Fig. 1*A*), we plot the difference variance: $\sigma^2 = \sigma^2_{NE} - \sigma^2_{DS}$ (or $\sigma^2 = \sigma^2_{GU} - \sigma^2_{DS}$) as a function of the concentration of NE (or GU) that induced the current. Fig. 1*B* shows that the difference variance of the fluctuations obeys the equation

$$\sigma^2 = \sigma^2_{max}[NE]^n/(K_M{}^n + [NE]^n),$$

where the dashed line is σ^2_{max} = 29 pA², K_M = 0.61 μM, and n = 0.9. At −120 mV and for concentrations up to 10 μM NE, the average values of the parameters are as follows: $\sigma^2_{max(NE)}$ = 31 ± 3 pA², $K_{M(NE)}$ = 0.60 ± 0.13 μM, and n_{NE} = 0.80 ± 0.15. GU-induced fluctuations follow a similar pattern with $\sigma^2_{max(GU)}$ = 25.0 ± 2.5 pA², $K_{M(GU)}$ = 0.61 ± 0.40 μM, and n_{GU} = 1.40 ± 0.15. Thus variance of the DS-sensitive fluctuations (σ^2) has approximately the same dependence on substrate concentration as the magnitude of the mean current (20). Furthermore, the variance of the induced fluctuations is unexpectedly large. For comparison, a cell resistance R of 1 GΩ would be expected to generate Johnson noise (31) in 2000 Hz bandwidth B of $\sigma^2_{Johnson} = 4kTB/R \approx 0.003$ pA². The

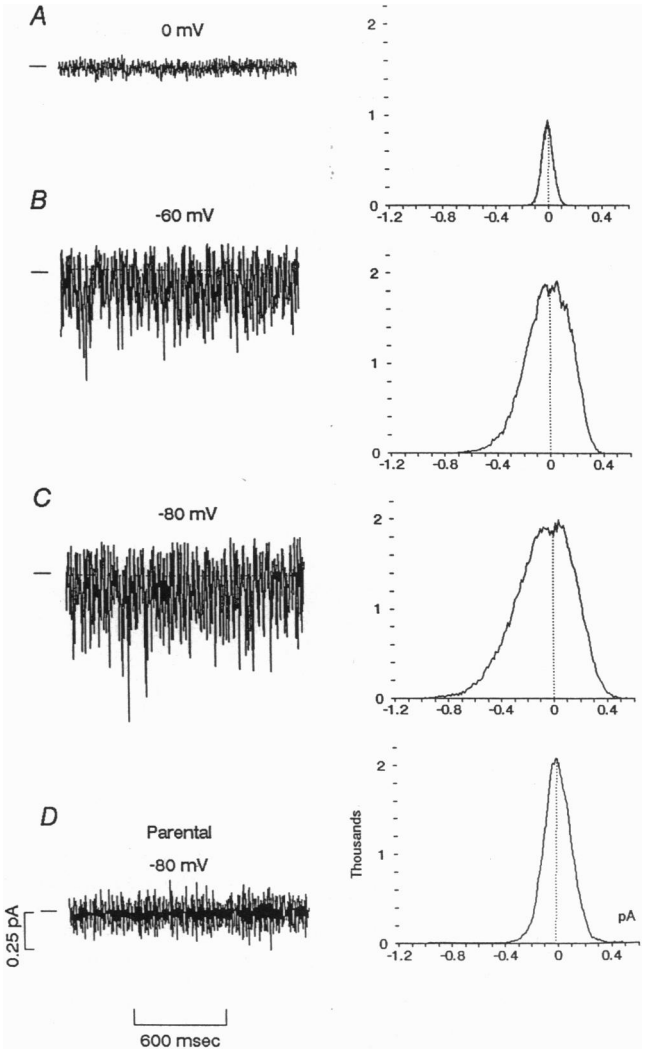

FIG. 2. Cell-attached patches. NE or GU induce current fluctuations in cell-attached patches on 293-hNET cells, and the inward deflections increase in amplitude with negative voltages. (*A*) A representative trace at 0 mV (absolute potential obtained by breaking the patch after the experiment to measure the cell resting potential, typically −40 mV). The pipette contained 30 μM GU. (*B* and *C*) The same patch at −60 and −80 mV. Amplitude histograms, shown to the right of each trace, are from 9 sec of data. In these histograms, the mean current was set arbitrarily to zero at each voltage. Similar data were obtained with 30 μM NE. The histograms in *A–C* show that in transfected cells with GU in the pipette (or NE, data not shown), patch noise has an asymmetric distribution of amplitudes that indicates the presence of inward channel-like openings. These openings are buried in the noise, but they are evident in the asymmetry of the traces and in the left asymmetry of the amplitude histograms. (*D*) A sample trace from similar experiment on a parental cell at −80 mV. The variance increases with voltage from 0.05 ± .011 pA² at 0 mV to 0.45 ± .04 pA² at −140 mV (four cells). In parental cells, however, with or without NE or GU in the pipette, patch noise has a symmetric distribution of amplitudes, as indicated in the histogram in *D*.

power spectral density of the fluctuations, $S_{NE}(f) - S_{DS}(f)$, is flat up to 2000 Hz. This implies that we cannot observe the true corner frequency of the events, because it is greater than the imposed bandwidth. However, the variance of the fluctuations can be used to estimate the magnitude of the underlying events.

Let us first estimate the magnitude of the charge underlying the fluctuations using shot noise theory. In this model each event is identical, and the net current generated by random "shots" depends on the charge q per shot and the rate r of

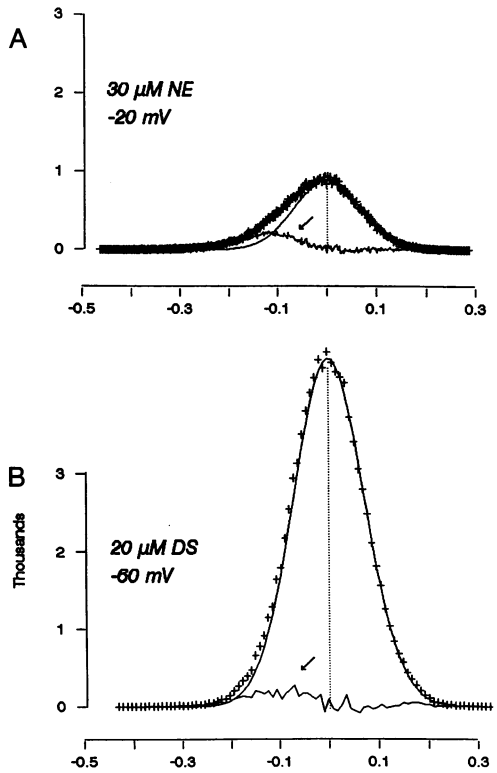

FIG. 3. Gaussian subtraction procedure. To extract the GU- or NE-induced inward current evident in Fig. 2 *A* and *B*, we first constructed a Gaussian curve that represents background. To construct the Gaussian, we use the right limb of the histogram and reflect it about the origin. This theoretical curve was then subtracted from the total histogram. After this procedure, the right limb of the histogram will obviously vanish. However, if the left limb is asymmetric with respect to the right, the procedure will reveal an underlying component. (*A*) Data from an inside-out patch taken from a transfected cell. It shows that even small asymmetries may be extracted from the total histogram by the Gaussian subtraction method. With 30 μM NE in the pipette and $V = -20$ mV across the patch, the asymmetric inward current represents a small fraction of the total amplitude (see also Fig. 2). The data are shown as dark crosses, the dotted vertical line through the peak is the axis of reflection for the theoretical Gaussian, and the solid curve is the constructed Gaussian. Subtracting the solid line from the data uncovers a minor component representing the inward fluctuations (arrow in Fig. 2*A*). At −20 mV, the peak of the inward component revealed by this procedure is −0.12 pA (2000 Hz bandwidth). (*B*) Same patch at a higher voltage (−60 mV), but after having added 20 μM DS to the bath (the cytoplasmic face of the patch). Although there is a substantial increase in the background current, there is virtually no asymmetric component in the presence of DS. Using the same procedure as above, the subtraction reveals essentially no inward component (arrow in Fig. 2*B*). In Fig. 4, we use Gaussian subtraction to measure the peak of the induced inward current at different voltages.

arrival of shots. In this case, the mean current is $I = Nqr$, which is the same formula used above to estimate the current expected from transport. In the present case, however, we allow q to be a free variable and determine its value from fluctuation analysis. The ratio of the variance of the fluctuations to the mean current is independent of the rate of arrival and allows us to estimate the charge that is transferred per event. If each event is a very brief pulse (approximately a delta function), and if we record fluctuations due to the random arrival of these events in the bandwidth B, then the ratio of the variance to the mean is given by the shot noise formula (31–33),

$$\sigma^2/I = 2qB.$$

Fig. 1*C* plots the measured ratio, σ^2/I, for a number of NE or GU concentrations. The plot shows that σ^2/I is essentially uncorrelated with [NE] or [GU]. An analysis of σ^2/I at −120 mV gives a mean ratio of 0.18 ± 0.04 pA for NE and 0.11 ± 0.02 pA for GU. The value of σ^2/I for the combined data is 0.145 ± 0.045 pA. Using the approximate value of 0.2 pA for σ^2/I, the charge transferred per event is

$$q \approx 0.5 \times 10^{-16} \text{ coul.}$$

Thus, ≈300 electronic charges make up each unitary event. Although a fixed-shot model could be consistent with the large NE-induced currents, even assuming turnover rates of one per second, we lack a physical model to account for a charge transfer of 300 e charges transport event.

If we assume instead that the transporter-associated events are ion channels with random open times, and if each event carries net current i with open probability p, then the variance-to-mean ratio formula becomes (31)

$$\sigma^2/I = i(1 - p).$$

In this formulation, the bandwidth does not appear explicitly. Nevertheless, the bandwidth imposes a restriction on observable events, namely, openings briefer than $1/2\pi(2000\text{Hz}) = 0.1$ msec cannot contribute significantly to the observed fluctuations (31). Assuming that the fluctuations are due to channels with random openings leads to the expression (Fig. 1*C*)

$$i(1 - p) \approx 0.2 \text{ pA}$$

for the NE-induced currents, and about half this magnitude for GU-induced currents (Fig. 1*C*). The experimental value, i = 0.2 pA, is furthermore a lower limit on the elementary current, because the probability is restricted by the formula $0 < p < 1$. Moreover, 0.2 pA is greater than we would expect for the transport of NE^+:Na^+:Cl^-: if we assume a charge of 1e and an open time at our limit of detection (0.1 msec), we predict an elementary current of 0.0016 pA, which is 130 times smaller than the current estimated from noise analysis. Shot noise analysis also predicted that the stoichiometric transport of NE^+, Na^+, and Cl^- would move <1% of the charge calculated to move in each shot.

The fluctuation analysis presented above suggests that we might expect to observe transporter-associated channels with currents in the range of 0.2 pA at −120 mV. Because of the imposed bandwidth, however, we would miss channel openings that are briefer than 0.1 msec. To look for such events, we performed experiments on transfected cells using the patch-clamp technique. Fig. 2 shows that the amplitude histogram of current fluctuations in cell-attached patches contains a left (inward) asymmetry. This inward component of the histogram becomes larger at negative membrane potentials (Fig. 2 *B* and *C*); furthermore, it is completely eliminated by 20 μM DS (data not shown), and it is absent in parental cells (Fig. 2*D*). To extract the amplitude of this inward component, we assumed that the total histogram is the sum of two Gaussians and used the subtraction procedure illustrated in Fig. 3. This analysis revealed that in cell-attached patches, at membrane potentials between −20 and −80 mV, the inward current varied linearly with voltage with a slope of 3.2 ± 0.4 pS ($n = 6$). Although this analysis suggests hNET-associated channels of the size predicted from whole-cell fluctuation analysis, we rarely observed channels as discrete events in cell-attached patches. Furthermore, the cell-attached configuration recordings may be compromised by changes in the cell resting potential. Inside-out patches offer a solution to these limitations (Fig. 4*A*). Removing the patch from the cell reveals distinct elementary events that are more easily resolved in amplitude histograms. These inward currents are blocked by 2 μM DS added to the bath to the inside face of the membrane (Fig. 4*B*, *Right*). Complete DS

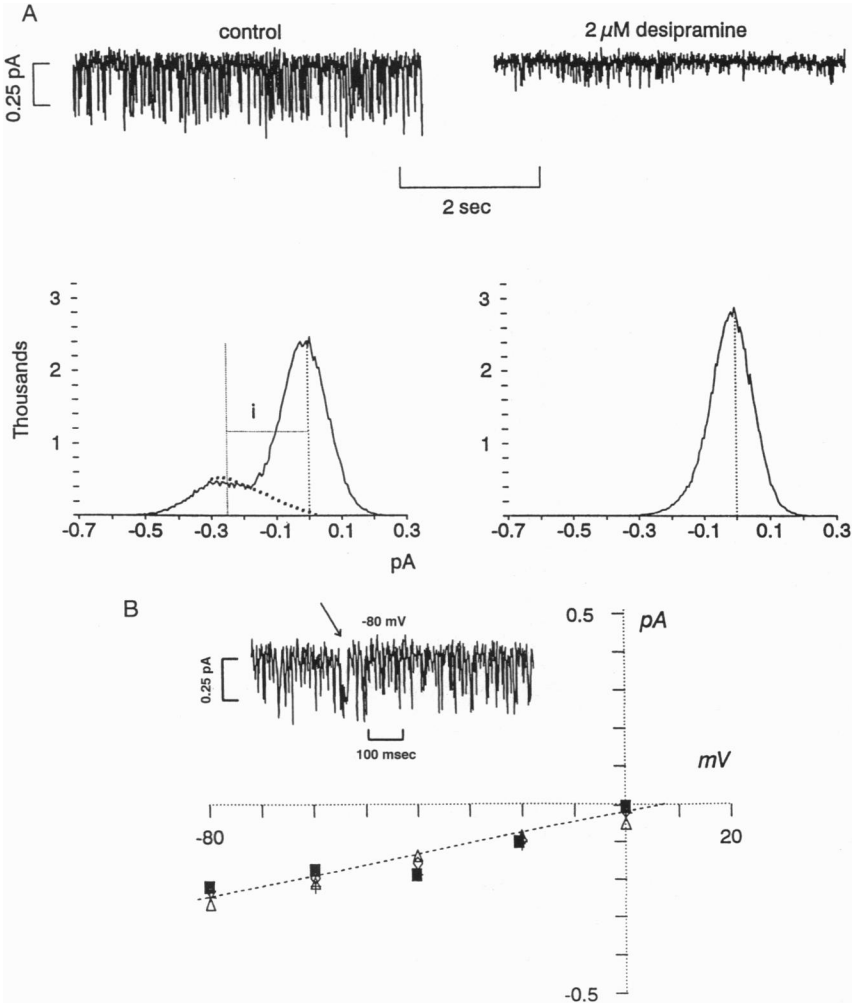

FIG. 4. Inside-out patches. GU induces channel-like activity in inside-out patches. (*A*, *Left*) Raw data and an amplitude histogram from an inside-out patch containing 30 μM GU (−80 mV). We used GU in these patch experiments to avoid complications of oxidation; furthermore, no GU receptors exist and the likelihood of false signals is less. Finally, although we obtained similar results with NE, GU gave more consistent events that were easier to analyze. At −80 mV, we can observe distinct inward current spikes. However, at voltages between 0 and -40 mV events are less visible. Thus we used the Gaussian subtraction procedure (Fig. 3) to quantify the GU-induced current at different voltages, even in those cases where single events are clear. The amplitude of the current at each voltage is defined as the center of the revealed inward component with respect to zero. This difference is shown as vertical dashed lines: in this example $i = -0.25$ pA. (*Right*) Same patch 1 min after adding 2 μM DS to the bath. At 1 min the block is incomplete, as indicated by inward spikes and the slight asymmetry in the histogram. Waiting up to 10 min, or using stronger concentrations of DS (20 μM), completely abolishes these inward currents. (*B*) $i(V)$ curve constructed by the method outlined in *A* (*Left*). At large negative voltages we can occasionally observe long openings; however, these were too inconsistent to quantify. The *inset* in the $i(V)$ curve shows an example of one of these rare, long events (arrow). The conductance defined by the Gaussian subtraction procedure in a bandwidth of 2000 Hz is linear in the range −20 to −80 mV with the value $\gamma_{hNET} = 2.95 \pm 0.17$ pS ($n = 4$).

block requires up to 10 min in 2 μM. As in cell-attached patches, this inward component of the patch currents is not present in parental cells. Although the elementary currents in inside-out patches appear more distinct than in cell-attached patches, long-lived events (see arrow, *Inset*) are rare. We therefore rely on the Gaussian subtraction procedure (Fig. 3) to measure the amplitude of the current. Fig. 4*B* shows that, for inside-out patches voltage clamped between 0 and −80 mV, the GU-induced inward current varies linearly with voltage and has a slope $\gamma = 2.95 \pm 0.17$ pS. We will refer to this hNET-associated conductance as the channel mode (C-mode) of conductance. In addition to induced currents, neurotransmitter transporters have well-documented leak currents (6, 7). We define leak through hNETs as the DS-sensitive current revealed in transfected cells independent of the presence of transmitter (20). On average, the leak current is only 10% of the induced current; thus it could be due to a smaller channel or the same channel at lower probability. We have attempted to find single-channel events linked to leak currents without success.

Because we observe discrete events with variable open times in cell-detached patches, we adopt the channel description for hNET-associated C-mode conduction. Two lines of evidence suggest that the probability of C-mode conduction is extremely low. For channels, the macroscopic current is given by $I = Nip$. Therefore, at a saturating transmitter concentration of 30 μM GU and at V = −80 mV,

$$Np \approx 100 \text{ pA}/0.2 \text{ pA} = 500.$$

Although we do not have an accurate measurement of N for a given cell, we can take the average number of [^{125}I]3β-[4-iodophenyl]tropan-2β-carboxylic acid methyl ester sites per transfected cell (20) as an approximation for N and estimate a value for p. For $N \approx 10^6$, then $p \approx 0.0005$. This means that, if the whole-cell current has the value 100 pA and if the underlying event is 0.2 pA, then the probability of C mode is the order of 0.5×10^{-3}. A more subtle argument involves the concentration dependence of I and of $i(1 - p)$. Our data show that whereas the whole-cell current, $I = Nip$, depends on [NE] or [GU] according to a Michaelis–Menten relationship (20), the variance-to-mean ratio, $\sigma^2/I = i(1 - p)$, is approximately independent of [NE] or [GU] (Fig. 1). For these data to be consistent, then the probability, p, must be much less than one. Considering these arguments, we propose the following description to encompass the voltage and concentration dependence of the macroscopic current and the current fluctuations for C-mode conduction in hNET:

$$I = Nip;$$

$$p = p_o[\text{NE}]/(K_M + [\text{NE}]);$$

$$\sigma^2 = Ni^2p(1 - p) \approx iI; \text{ and}$$

$$i = \gamma(V - E),$$

where $\gamma = 3$ pS, $E = +Bmr$, $K_M = 0.6$ μM, and p_o is the order of 10^{-3}. The factor p_o is the upper bound for the probability of C-mode conduction and states that, even under saturation conditions, C-mode occurs only 0.1% of the time.

From a comparison of NE transport and NE-induced current, we estimated that at negative voltages, ≈300 charges cross the membrane for each molecule of NE transported. Furthermore, shot noise analysis indicated that ≈300 electronic charges make up each unitary event. A similar analysis of the noise as channel activity gave ≈130 electronic charges per event. Thus the electrical events occur with about the same frequency as transport. While this may be coincidence, it is also possible that the transporter opens as a transmembrane ion channel every time it transports NE.

Finally, we note that the parameter p_o, which is the maximum value for the probability of opening, may be different for different substrates. We have shown that under similar conditions of transmitter-induced current, $I_{(GU)} > I_{(NE)}$. A congruous explanation would be that $p_o(GU) > p_o(NE)$. In other words, GU is more effective than NE at opening the channel. Once the channel is open, however, the current is the same for either substrate. This model explains transmitter uptake measured by radioligands, the Michaelis–Menten dependence of NE- and Na-induced current, the voltage dependence of the induced current, the concentration dependence of the induced current, the magnitude of the whole-cell current, and the magnitude of the current fluctuations.

These experiments demonstrate that hNETs that have both transporter modes and C-modes of conduction. A Michaelis–Menten analysis of uptake and substrate-induced currents indicates Hill coefficients for NE (or GU) and Na near $n = 1$ (20). In addition, hNET requires one Cl ion for NE transport (7), and recently the ion coupling stoichiometry for hNETs that we have assumed in this paper has been confirmed (34). These data suggest that although transporter mode is electrogenic, it generates negligible current. Indeed, 10^6 hNETs transporting a net charge of 1 e at rate of one per second would generate a current of only 0.16 pA. Although the probability of any given channel being open is low, C-mode carries the majority of the current. Our conclusion that C-mode dominates NE-induced current in hNETs does not generalize to other cotransporters. In mammalian serotonin transporters, which are reported to be electroneutral (19), the serotonin-induced current and the number of seratonin molecules transported are in approximate agreement (24). However, in glutamate transporters, although C-mode is present, the majority of current can be carried in transporter mode (35). Furthermore, the relative contributions of transporter mode and C-mode may vary even among homologues of these transporters (27). Does C-mode conduction exist in native preparations? No evidence of this type exists for NE transporters. A large current is associated with serotonin uptake in *Hirudo* neurons (22); however, the number and turnover rate of these transporters is unknown. Evidence for C-mode in a native preparation comes from noise analysis, which has revealed channel behavior in glutamate transporters in salamander photoreceptors (36).

If hNET combines the properties of a classical cotransporter with a transmitter-gated ion channel, as our data suggest, questions arise concerning the consequences of this behavior for transporter function. Is transport necessary to stimulate channel activity? Is C-mode an obligate step in gating amine flux? Must the substrate bind to open the channel? Does the same pore that carries the majority of the current carry the neurotransmitter? Finally, does C-mode exist in native tissue, and, if so, what are the consequences of the currents associated with hNET for neural transmission? These questions await further investigation. Certainly a greater time resolution of hNET-associated events has been achieved, offering a new approach for investigations into transporter mechanisms and regulation. Properties of NET revealed in detached patches also offers new paradigms to relate substrate and drug binding to the structural features of NET proteins.

The authors wish to thank Gary Rudnick for useful discussion, B. J. Duke for developing and maintaining the cell lines used in this study and preparing the solutions, and Alex Daniel and Bill Goolsby for computer and electronics support. This research was supported by National Institutes of Health Grant HL-27388 and Emory University Research Grant 2-50763 to L.J.D., and National Institutes of Health Grants NS-33373 and DA-07390 and a Mallinckrodt Award to R.D.B.

1. Amara, S. & Kuhar, M. J. (1993) *Annu. Rev. Neurosci.* **16,** 73–93.
2. Barker, E. & Blakely, R. D. (1995) in *Psychopharmacology: The Fourth Generation of Progress,* eds. Bloom, F. E. & Kupfer, D. J. (Raven, New York), pp. 321–333.
3. Nirenberg, M. J., Vaughan, R. A., Uhl, G. R. Kuhar, M. J. & Pickle, V. M. (1996) *J. Neurosci.* **16,** 436–447.
4. Clarkson, C. W., Chang, C., Stolfi, A., George, W. J., Yamasaki, S. & Pickoff, A. S. (1993) *Circulation* **87,** 950–962.
5. Rudnick, G. & Clark, J. (1993) *Biochim. Biophys. Acta* **1144,** 249–263.
6. Lester, H. A. Mager, S., Quick, M. W. & Corey, J. L. (1994) *Annu. Rev. Pharmacol. Toxicol.* **34,** 219–249.
7. Blakely, R. D., DeFelice, L. J. & Hartzell, H. C. (1994) *J. Exp. Biol.* **196,** 263–281.
8. Hertting, G., Axelrod, J., Kopin, I. J. & Whitby (1961) *Nature (London)* **189,** 66–69.
9. Axelrod, J., Whitby, L. G. & Hertting, G. (1961) *Science* **133,** 383–384.
10. Whitby, L. G. & Axelrod, J. (1961) *J. Pharmacol. Exp. Ther.* **132,** 193–201.
11. Axelrod, J. (1971) *Science* **173,** 598–603.
12. Iversen, L. L. & Kravitz, E. A. (1966) *Mol. Pharmacol.* **2,** 360–362.
13. Sanchez-Armass, S. & Orrego, F. (1977) *Life Sci.* **20,** 1829–1838.
14. Sammet, S. & Graefe K. H. (1979) *Arch. Pharmacol.* **309,** 99–107.
15. Harder, R. & Bonisch, H. (1985) *J. Neurochem.* **45,** 1154-1162.
16. Bonisch, H. & Harder, R. (1986) *Arch. Pharmacol.* **334,** 403–411.
17. Friedrich, U. & Bonisch, H. (1986) *Arch. Pharmacol.* **333,** 246–252.
18. Ramamoorthy, S., Prasad, P., Kulanthaivel, P., Leibach, F. H., Blakely, R. D. & Ganapathy, V. (1993) *Biochemistry* **32,** 1346–1353.
19. Gu, H., Wall, S. C. & Rudnick, G. (1994) *J. Biol. Chem.* **269,** 7124–7130.
20. Galli, A., DeFelice, L. J., Duke, B. J., Moore, K. R. & Blakely, R. D. (1995) *J. Exp. Biol.* **198,** 2197–2212.
21. Malchow, R. P. & Ripps, H. (1990) *Proc. Natl. Acad. Sci. USA* **87,** 8945–8949.
22. Bruns, K. J., Engert, F. & Lux, H. D. (1993) *Neuron* **10,** 559–572.
23. Mager, S., Naeve, J., Quick, M., Guastella, J., Davidson, N. & Lester, H. A. (1993) *Neuron* **10,** 177–188.
24. Mager, S., Min, C., Henry, D., Chavkin, C., Hoffman, B. Davidson, N. & Lester, H. A. (1994) *Neuron* **12,** 11–20.
25. Cammack, J. N., Rakhilin, S. V. & Schwartz, E. A. (1994) *Neuron* **13,** 949–960.
26. Risso, S., DeFelice, L. J. & Blakely, R. D. (1995) *J. Physiol. (London)* **490,** 691–702.
27. Fairman, W. A., Vandenberg, R. I., Arriza, J. L. Kavanaugh, M. P. & Amara, S. G. (1995) *Nature (London)* **375,** 599–602.
28. Cammack, J. N. & Schwartz, E. A. (1996) *Proc. Natl. Acad. Sci. USA* **93,** 723–727.
29. Pacholczyk, T., Blakely, R. D. & Amara, S. G. (1991) *Nature (London)* **350,** 350–354.
30. Melikian, H. E., McDonald, J. K., Gu, H., Rudnick, G., Moore, K. R. & Blakely, R. D. (1994) *J. Biol. Chem.* **269,** 12290–12297.
31. DeFelice, L. J. (1981) *Introduction to Membrane Noise* (Plenum, New York).
32. Läuger, P. (1984) *Eur. Biophys. J.* **11,** 117–128.
33. Crouzy, S. C. & Sigworth, F. J. (1993) *Biophys. J.* **64,** 68–76.
34. Howard, H., Wall, S., Rudnick, G. (1996) *J. Biol. Chem.*, in press.
35. Wadiche, J. I., Amara, S. G. & Kavanaugh, M. P. (1995) *Neuron* **15,** 721–728.
36. Larson, H. P., Picaud, S. A., Werblin, F. S. & Lecar, H. (1996) *Biophys. J.* **70,** 733–742.